Progress In Electromagnetics Research B, Vol. 7, 209–222, 2008

TEMPERATURE DEPENDENCE ANALYSIS OF THE CHROMATIC DISPERSION IN WII-TYPE ZERO-DISPERSION SHIFTED FIBER (ZDSF)

A. Rostami [†] **and S. Makouei**

Photonics and Nanocrystals Research Lab. (PNRL)
Faculty of Electrical and Computer Engineering
University of Tabriz
Tabriz 51664, Iran

Abstract—In this paper, we design the zero-dispersion wavelength shifted fiber based on the WII-type triple clad single mode optical fiber and consider the transmission parameters fluctuations owing to environmental conditions such as temperature variations on dispersion behavior of fiber. In order to estimate the thermal coefficients, the model introduced by Ghosh [1] is applied. Our calculation show that the thermal coefficient extracted for the chromatic dispersion, its slope, and the zero dispersion wavelength swing are -1.21×10^{-3} ps/km/nm/°C, $+2.96\times10^{-3}$ ps/km/nm^2/°C, and $+3.33\times10^{-2}$ nm/°C at 1.55 μm respectively. It is shown that in optical fiber design especially for dense wavelength division multiplexing (DWDM) systems, effect of temperature on channel displacement is critical and should be considered carefully.

1. INTRODUCTION

The optical fiber communication is the basic and appropriate alternative for high speed data transmission nowadays. The optical silica fiber might be the only proper choice for this task. Considering high-speed data transmission through silica fiber, there are some disadvantages including chromatic dispersion and its slope. Meanwhile, these two factors cause severe restrictions for the high speed pulse propagation. Zero-dispersion wavelength communication is the first option. In the fiber design shifting the zero-dispersion

[†] Also with School of Engineering Emerging Technologies, University of Tabriz, Tabriz 51664, Iran

wavelength to a wavelength in which the fiber has minimum attenuation is preferred [2] too. This approach allows minimizing the pulse broadening factor and consequently makes the long distance communication feasible.

It is apparent that the transmission performances are manipulated and optimized by controlling the optical and geometrical parameters in the fiber structures. As a result, any undesired variation in the fiber structure parameters, can perturb the transference performances. The refractive index variation as a function of temperature (dn/dT) is the important feature in the optical fibers. This factor determines the temperature characteristics of an optical fiber transmission system. Aerial optical systems are expected to face changes of temperature in several areas of the planet, which compel the essential demand to contemplate the thermal effect in the design of high speed optical communication systems.

The study of the temperature dependence of the Sellmeier coefficients has been done by Gosh et al. [3]. Temperature-dependent Sellmeier coefficients are necessary to optimize optical design parameters of the optical fiber transmission system. They have found out that the zero dispersion wavelength varies linearly with temperature and $d\lambda_0/dT$ is $0.025\,\mathrm{nm/^\circ K}$ at $\lambda_0 = 1.273\,\mu\mathrm{m}$.

The refractive index thermal coefficient has been analyzed, by Gosh [1], for three optical fiber based glasses in a physically meaningful model for the first time to compute refractive indexes at any operating temperature and wavelength. He believes that the energy gap corresponding to the peak position of the electronic absorption which lies in the ultra violet (VUV) spectral region is the major contributor to the dispersion of thermo-optic coefficients of these glasses.

Two models for the chromatic dispersion and its slope variations with temperature have been developed by Andre et al. [4]. It has been shown that for systems operating at 40 Gbit/s and above, temperature impacts have to be considered in design.

In the paper reported by Zhang et al. [5], the characteristics of the chromatic dispersion and its slope were discussed in detail, but there is no attention on the dispersion fluctuations owing to environmental conditions. Also the dispersion and its slope estimations are done numerically.

Recently, Rostami et al. [6] have stabilized the analytical approach to calculate these parameters. Due to analytically based relationships, this approach accurately covers all the numerical method presented so far. For a case study, the given analytical method is used to analyze the M-type fiber structure.

In [7], the authors have introduced a novel design method to

control the chromatic dispersion and its slope simultaneously. Their proposal is based on the Genetic Algorithm by adjusting a special fitness function for desired aims.

Also, there are different design methods for management of dispersion in multi-clad optical fiber [8]. In these methods optimization algorithm with different fitness functions were examined. Nonlinear effects in fiber optics were discussed in [9].

Dispersion management especially in optimized case was discussed in [10, 11]. In these papers a mathematical tool for optimum dispersion compensation was developed. But in this investigation effect of temperature was ignored.

Finally effect of crosstalk and reduction in multiplexed fiber optic communication system was considered in [12].

In this paper, using the method presented in [7], we design the zero-dispersion wavelength shifted fiber based on the WII-type triple clad single mode optical fiber and consider the transmission parameters fluctuations due to environmental conditions such as temperature variations. In order to estimate the thermal coefficients, the model introduced in [1] is applied. Meanwhile, the dispersion and its slope are computed using the analytical approach presented in [6].

The following organization for description of temperature effect on dispersion factor is done and presented in detail.

In Section 2, the modal analysis of the proposed structure is done with details and the paper is followed by the dispersion and its slope computations. Then the temperature dependence of the refractive indexes is concerned in Section 4. Simulation result and discussion is presented in Section 5. Finally the paper ends with a short conclusion.

2. MODAL ANALYSIS

The modal analysis based on the LP approximation is presented in this section for the proposed structure illustrated in Fig. 1.

The index of refraction is defined as follows in this structure.

$$n(r) = \begin{cases} n_1, & 0 < r < a, \\ n_2, & a < r < b, \\ n_3, & b < r < c, \\ n_4, & c < r, \end{cases} \tag{1}$$

where r is the radius position of optical fiber. According to the LP approximation to calculate the electrical field distribution, there are two regions of operation which can be defined as follows.

$$I: \ n_4 < n_{eff} < n_3 \quad II: \ n_3 < n_{eff} < n_1 \tag{2}$$

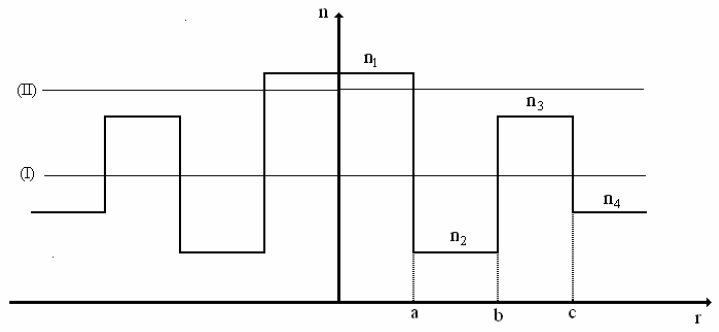

Figure 1. The refractive index profile for the proposed structures (WII).

The guided modes and propagation wave vectors can be obtained by using two determinants (Eqs. (3), (4)) which are constructed by the boundary conditions. The two lines drawn in Fig. 1 demonstrate these two operation regions. The effective refractive index is given by $n_{eff} = \beta_g/k_0$, where β_g is the longitudinal propagation constant of the guided modes and k_0 is the wave number in vacuum.

$$\begin{vmatrix} J_m(U_1) & -I_m(W_3) & -K_m(W_3) & 0 & 0 & 0 \\ 0 & I_m(\overline{W_3}) & K_m(\overline{W_3}) & -J_m(U_3) & -Y_m(U_3) & 0 \\ 0 & 0 & 0 & J_m(\overline{U_3}) & Y_m(\overline{U_3}) & -K_m(W_4) \\ U_1 J'_m(U_1) & -W_3 I'_m(W_3) & -W_3 K'_m(W_3) & 0 & 0 & 0 \\ 0 & \overline{W_3} I'_m(\overline{W_3}) & \overline{W_3} K'_m(\overline{W_3}) & -U_3 J'_m(U_3) & -U_3 Y'_m(U_3) & 0 \\ 0 & 0 & 0 & \overline{U_3} J'_m(\overline{U_3}) & \overline{U_3} Y'_m(\overline{U_3}) & -W_4 K'_m(W_4) \end{vmatrix} = 0, \quad (n_4 < n_{eff.} < n_3), \tag{3}$$

$$\begin{vmatrix} J_m(U_1) & -I_m(W_3) & -K_m(W_3) & 0 & 0 & 0 \\ 0 & I_m(\overline{W_3}) & K_m(\overline{W_3}) & -I_m(U_2) & -K_m(U_2) & 0 \\ 0 & 0 & 0 & I_m(\overline{U_2}) & K_m(\overline{U_2}) & -K_m(W_4) \\ U_1 J'_m(U_1) & -W_3 I'_m(W_3) & -W_3 K'_m(W_3) & 0 & 0 & 0 \\ 0 & \overline{W_3} I'_m(\overline{W_3}) & \overline{W_3} K'_m(\overline{W_3}) & -U_2 I'_m(U_2) & -U_2 K'_m(U_2) & 0 \\ 0 & 0 & 0 & \overline{U_2} I'_m(\overline{U_2}) & \overline{U_2} K'_m(\overline{U_2}) & -W_4 K'_m(W_4) \end{vmatrix} = 0, \quad (n_3 < n_{eff.} < n_1), \tag{4}$$

where, the appeared transversal propagation constants are given as

follows.

$$\begin{aligned} U_1 &= a\sqrt{k_0^2 n_1^2 - \beta^2}, \\ W_3 &= a\sqrt{\beta^2 - k_0^2 n_2^2}, \quad \overline{W_3} = \frac{P}{Q} W_3, \\ U_2 &= b\sqrt{\beta^2 - k_0^2 n_3^2}, \quad \overline{U_2} = \frac{1}{P} U_2, \\ U_3 &= b\sqrt{k_0^2 n_3^2 - \beta^2}, \quad \overline{U_3} = \frac{1}{P} U_3, \\ W_4 &= c\sqrt{\beta^2 - k_0^2 n_4^2}. \end{aligned} \tag{5}$$

Also, for easy handling of the problem the following optical parameters are defined as follows.

$$R_1 = \frac{n_1 - n_3}{n_3 - n_2}, \quad R_2 = \frac{n_2 - n_4}{n_3 - n_2}, \quad \Delta = \frac{n_1^2 - n_4^2}{2n_4^2} \approx \frac{n_1 - n_4}{n_4}. \tag{6}$$

For this structure the geometrical parameters are introduced as follows:

$$P = \frac{b}{c}, \quad Q = \frac{a}{c}. \tag{7}$$

The following constants are defined as

$$q_1 = \frac{1 + R_1}{1 + R_1 + R_2}, \quad q_2 = \frac{R_1}{1 + R_1 + R_2}. \tag{8}$$

Finally the normalized frequency and wave vector are given as

$$V = k_0 a\sqrt{n_1^2 - n_4^2}, \quad B = \frac{(\beta/k_0)^2 - n_4^2}{n_1^2 - n_4^2} = 1 - \left(\frac{U_1}{V}\right)^2. \tag{9}$$

3. DISPERSION AND DISPERSION SLOPE ANALYSIS

In this section dispersion and dispersion slope analysis based on derived relations in previous section including waveguide and material dispersions (single mode fibers) are done. So, for the proposed structure total dispersion and dispersion slope are given in Eq. (10) and Eq. (11) respectively.

$$D = -\frac{\lambda}{c}\frac{d^2 n_4}{d\lambda^2}\left[1 + \Delta\frac{d(VB)}{dV}\right] - \frac{N_4}{c}\frac{\Delta}{\lambda} V\frac{d^2(VB)}{dV^2}, \tag{10}$$

$$S = -\frac{\lambda}{c}\frac{d^3 n_4}{d\lambda^3}\left[1+\Delta\frac{d\,(VB)}{dV}\right] - \frac{1}{c}\frac{d^2 n_4}{d\lambda^2}\left[1+\Delta\frac{d\,(VB)}{dV}\right] + \frac{N_4}{c}\left(\frac{\Delta}{\lambda^2}\right)V^2\frac{d^3\,(VB)}{dV^3} + 2\frac{N_4}{c}\frac{\Delta}{\lambda^2}V\frac{d^2\,(VB)}{dV^2} + 2\frac{\Delta}{c}\frac{d^2 n_4}{d\lambda^2}V\frac{d^2\,(VB)}{dV^2}, \quad (11)$$

where $N_4 = n_4 - \lambda(dn_4/d\lambda)$ is the group index of the outer cladding layer. Also, the Sellmeier formula can be used for calculation of material dispersion ($dn_4/d\lambda$ and $d^2n_4/d\lambda^2$). For complete calculation of Eq. (10) and Eq. (11), $d(VB)/dV$, $Vd^2(VB)/dV^2$, and $V^2d^3(VB)/dV^3$ must be calculated.

For this purpose Eq. (3), (4) and the following equations can be used.

$$\frac{d\,(VB)}{dV} = 1 + \left(\frac{U_1}{V}\right)^2\left(1 - 2\frac{V}{U_1}\frac{dU_1}{dV}\right), \quad (12)$$

$$V\frac{d^2\,(VB)}{dV^2} = -2\left(\frac{dU_1}{dV} - \frac{U_1}{V}\right)^2 - 2U_1\frac{d^2U_1}{dV^2}, \quad (13)$$

$$V^2\frac{d^3\,(VB)}{dV^3} = 6\left(\frac{dU_1}{dV} - \frac{U_1}{V}\right)^2 - 2U_1V\frac{d^3U_1}{dV^3} - 6V\frac{d^2U_1}{dV^2}\left(\frac{dU_1}{dV} - \frac{U_1}{V}\right), \quad (14)$$

To complete calculation of total dispersion and dispersion slope, estimation of Eq. (12), Eq. (13), and Eq. (14) are necessary. For this purpose, the essential calculations to obtain the dispersion and its slope relationships are done according to the method introduced and explained completely by Rostami et al. [6]. Due to analytically based relationships, this approach accurately covers all the numerical method reported so far.

4. THE TEMPERATURE DEPENDENCE OF THE REFRACTIVE INDEXES

The refractive index variation due to temperature is considered in this section. The method used in this paper has been introduced by Ghosh [1]. This model is based on the subscription of both electrons and optical phonons. The optical constants computed from this model are then used to calculate the refractive indexes at any operating

temperature or wavelength for the optical fiber transmission system. Thermo-optic coefficient dn/dT contains the contribution of electrons and optical phonons. Consequently, it can be described in the optical transmission range in terms of linear expansion coefficient α and the temperature variation of energy gap (dE_g/dT) by the following relation as [13]

$$2n\,(dn/dT) = \chi_e \left[-3\alpha - \frac{2}{E_g} \cdot \frac{dE_g}{dT} \cdot \frac{E_g^2}{\left(E_g^2 - E^2\right)}\right], \tag{15}$$

where n, χ_e, E, and E_g are the room temperature refractive index, the electronic susceptibility, photon energy, and the suitable energy gap lying in the vacuum ultraviolet region respectively. The above equation can be rewritten in terms of a normalized wavelength $R = \lambda^2/(\lambda^2 - \lambda_g^2)$ as

$$2n\left(\frac{dn}{dT}\right) = GR + HR^2, \tag{16}$$

where the constants G and H are related respectively to the thermal expansion coefficient (α) and the energy gap temperature coefficient (dE_g/dT) according to the relations presented in [1] and their values are given in Table 1 for silica glasses. Meanwhile the curve obtained using these parameters are illustrated in Fig. 2.

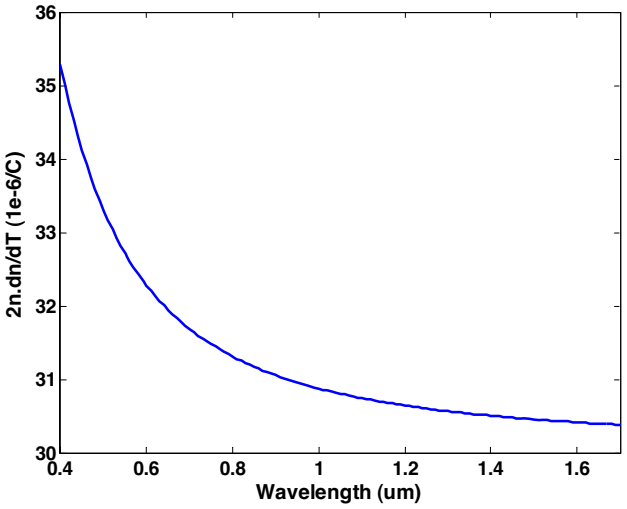

Figure 2. $2n.dn/dT$ versus wavelength.

This figure shows that the thermo-optic coefficient is nearly constant and positive in the $S + C + L$ telecommunication bands [14]. In the meantime, the refractive index is strongly fluctuated near the electronic absorption edge.

Table 1. Interpolated coefficient in the relation $2n.dn/dT = GR + HR^2$.

G ($10^{-6/^\circ}$)	H ($10^{-6/^\circ}$)	λ_g (μm)	α ($10^{-6/^\circ}$)
−1.6548	31.7794	0.109	0.45

5. SIMULATION RESULTS AND DISCUSSION

In order to study the temperature dependence of the transmission characteristics of the optical fiber, we have concentrated on the zero-dispersion wavelength shifted fiber based on the WII-type optical fiber. The ZDSF structure has been designed using the method which is completely described in [7]. It should be kept in mind that in the fiber design, one likes to shift the zero-dispersion wavelength to the region that the fiber has the lowest level attenuation. The optical attenuation has a global minimum around 1.55 μm wavelength and that is why the most optical communication systems are operated at this wavelength. Seeing that, the λ_0 and σ parameters of the method presented in [7] are set to 1.55 μm and 0.0 to achieve the desired structure. In other words, the pulse broadening factor, which is the key function in the design approach, is optimized in the λ_0 single wavelength. The calculated optical and geometrical parameters in the designed fiber structure are listed in Table 2.

Table 2. The optical and geometrical parameters for the designed fiber structure.

a (μm)	P	Q	R_1	R_2	Δ
2.2225	0.8917	0.3823	6.6099	−0.1365	8.8210e-3

Due to the refractive index thermo-optic coefficient and the thermal expansion coefficient, the optical and geometrical parameters are altered. It must be mentioned that the optical transmission characteristics of the optical fiber such as the dispersion, its slope, and pulse broadening factor are changed by any variation in amount of the parameters listed in Table 2.

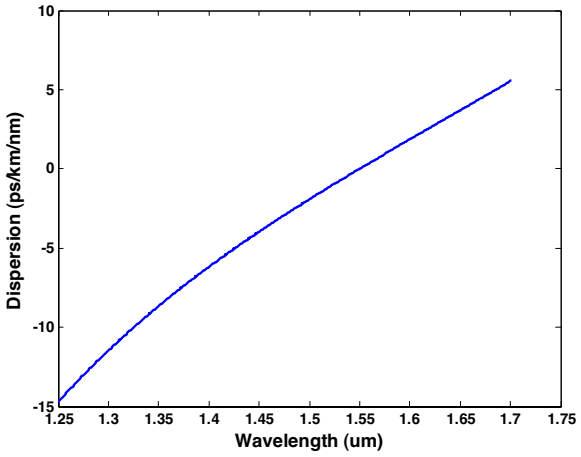

Figure 3. Dispersion vs. wavelength.

In the beginning, the chromatic dispersion and its slope characteristics are examined as a function of temperature. From Fig. 3, it is observed that the zero-dispersion wavelength is precisely adjusted at λ_0 which is equal to 1.55 µm at the room temperature. The calculated results show that the amount of dispersion and its slope are 1.7394×10^{-4} ps/km/nm and 0.03769 ps/km/nm^{2}respectively which are so appropriate in the case of ZDSF applications.

It must be taken into account that the optical and geometrical parameters of the designed fiber are sensitive to temperature. As a result, any variation in the temperature can move the zero-dispersion wavelength, which is severely related to the fiber structure, toward the higher or lower wavelength. Fig. 4 shows the temperature alteration effect on the chromatic dispersion value at 1.55 µm. With attention to the Fig. 4 it can be found out that the chromatic dispersion amount increases and decreases by any negative and positive change in the temperature respectively. A value of -1.21×10^{-3} ps/km/nm/°C is obtained for the chromatic dispersion thermal coefficient at 1.55 µm (dD/dT). Meanwhile, the obtained coefficient can be used for the chromatic dispersion in the $S + C + L$ telecommunication bands due to the low slope of $2n.dn/dT$ curve in these wavelengths. We have also estimated the dispersion slope thermal coefficient like above. The value for this parameter is calculated $+2.96 \times 10^{-3}$ ps/km/nm^2/°C at 1.55 µm (dS/dT).

As the other investigation, we can focus on the zero dispersion wavelength variation which is demonstrated in Fig. 5. It is clear that the zero dispersion wavelength moves toward the higher wavelength

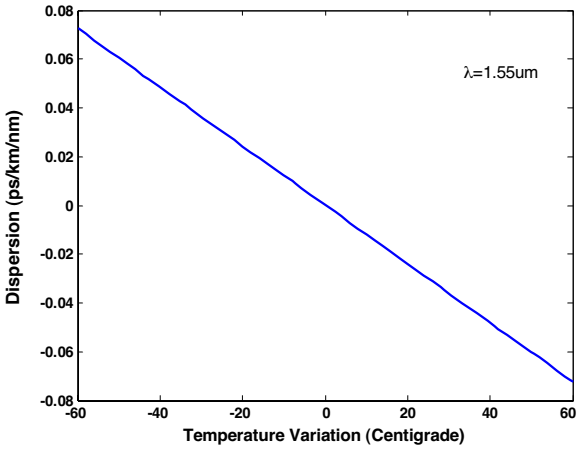

Figure 4. Dispersion vs. temperature variation at $\lambda = 1.55\,\mu$m.

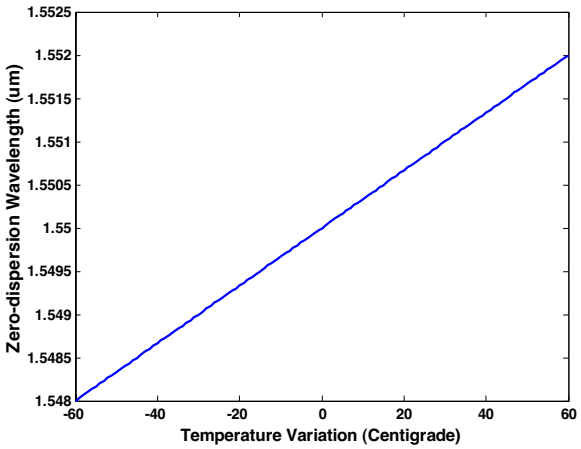

Figure 5. Zero-dispersion wavelength vs. temperature variations.

by the temperature raising. It can be explained considering the variation of Δ parameter due to the temperature displacements. A brief glance on Fig. 2 exhibits that the refractive index thermal coefficient is positive. As a result, the Δ optical parameter increases by the temperature increasing. It is shown by Zhang et al. [5] that this variation of Δ shifts the zero-dispersion wavelength to higher wavelengths. The value of $+3.33 \times 10^{-2}\,\mathrm{nm/^{\circ}C}$ is extracted for the zero-dispersion wavelength thermal coefficient ($d\lambda_0/dT$).

As said earlier, the ZDSF is designed by optimizing the pulse

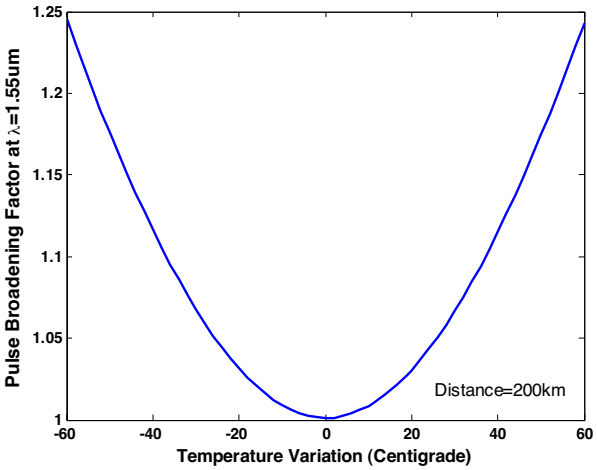

Figure 6. Pulse broadening factor vs. temperature variation at $\lambda = 1.55\,\mu$m.

broadening factor. In this simulation the Gaussian un-chirped initial pulse with 5 ps full-width at half-maximum is used. It is useful to mention that the distance parameter is set at 200 km. Owing to the dispersion and its slope variation, the fluctuation of pulse broadening factor as a function of temperature is anticipated. The calculated results indicate that the broadening factor is increased to 1.0012 after 200 Km propagation at 1.55 µm which is excellent for practical cases. In other words, the pulse width is expanded only 0.12% after 200 Km traveling. Fig. 6 is illustrated to show the influence of the temperature variation on the pulse broadening factor at 1.55 µm. Due to the symmetric changes at dispersion and its slope at 1.55 µm, temperature increasing and decreasing has nearly identical impression on this factor. It is clear that the pulse becomes broader by any temperature variations. For example, if we have a growth of 26°C, the pulse width will be enlarged 5% after 200 Km traveling. It is obvious that the temperature fluctuation effect on the foregoing factor is more serious than the dispersion and its slope.

In the following, the dispersion and higher order dispersion lengths of the proposed structure are obtained and the temperature impact on the structure is examined. In addition of the pulse broadening factor, these characteristics are used to evaluate the long haul communication performances. Meanwhile, these quantities are defined to investigate the effectiveness of the dispersion properties of the designed optical fibers. According to these definitions, the following relationships are

given to extract the dispersion and higher order dispersion lengths respectively [15].

$$L_D = \frac{t_i^2}{|\beta_2|}, \tag{17}$$

$$L'_D = \frac{t_i^3}{|\beta_3|}, \tag{18}$$

where t_i is the initial Gaussian pulse full-width at half-maximum. The mathematical relationship for β_2 and β_3 are given as follows.

$$\beta_2 = \frac{d^2}{d\omega^2}\beta(\omega)\,|_{\omega=\omega_c}\,, \tag{19}$$

$$\beta_3 = \frac{d^3}{d\omega^3}\beta(\omega)\,|_{\omega=\omega_c} = \left(S - \frac{4\pi c}{\lambda^3}\beta_2\right)\frac{\lambda^4}{(2\pi c)^2}, \tag{20}$$

where S and c are the dispersion slope and the light speed in the vacuum respectively. The dispersion length at 1.55 μm as a function of temperature variation is shown in Fig. 7. From Eqs. (17), (19), it is clear that this parameter is strongly related to the chromatic dispersion value. As a result, any changes at temperature and consequently dispersion value, decreases the dispersion length. But the case is a little

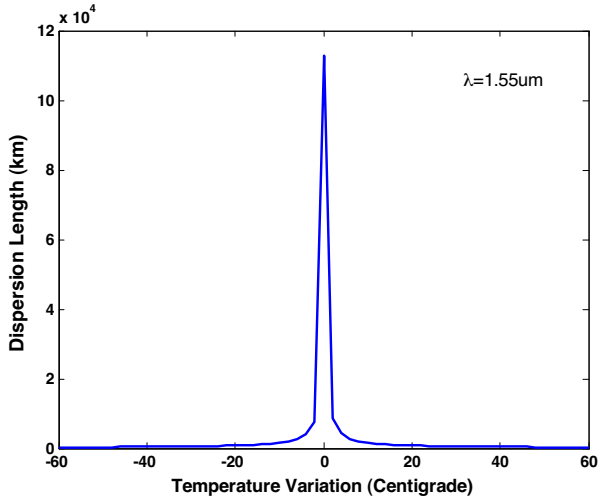

Figure 7. The dispersion length vs. temperature variation at $\lambda = 1.55\,\mu$m.

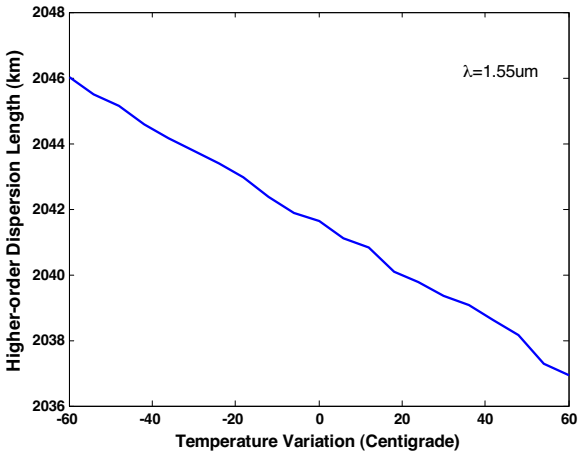

Figure 8. The higher-order dispersion length vs. temperature variation at $\lambda = 1.55\,\mu$m.

complicated about the higher order dispersion length. This parameter is related to β_2 and β_3 simultaneously which show the dispersion and its slope influences respectively. When temperature has negative drift, the dispersion slope value decreases and its reduction is firmer than the dispersion increasing. Consequently the higher order dispersion length faces to growth by decreasing the temperature. Meanwhile, the origin of this outcome is the opposite sign of the thermal coefficient evaluated in the dispersion and its slope cases.

In this section simulation result of the considered structure from dispersion behavior point of view due to variation of the temperature was studied. It was shown that variation of temperature has critical effect on fiber optic network operation. So, it should be considered in fiber design strategy.

6. CONCLUSION

The optical transmission responses of the designed ZDSF were evaluated as a function of temperature. It was found out that this environmental factor must be considered in the desired optical fiber design. The calculated thermal coefficients for the chromatic dispersion (dD/dT) and its slope (dS/dT) are respectively -1.21×10^{-3} ps/km/nm/°C and $+2.96\times10^{-3}$ ps/km/nm^2/°C at 1.55 µm. In the meantime, in the case of the zero-dispersion wavelength, the computed value for its thermal coefficient ($d\lambda_0/dT$) is $+3.33 \times 10^{-2}$ nm/°C at the mentioned wavelength.

REFERENCES

1. Ghosh, G., *Photonics Technology Letters*, Vol. 6, 431, 1994.
2. Li, Y. W., C. D. Hussey, and T. A. Briks, *Lightwave Technology*, Vol. 1, 1812, 1993.
3. Gosh, G., M. Endo, and T. Iwasaki, *Lightwave Technology*, Vol. 12, 1338, 1994.
4. Andre, P. S. and A. N. Pinto, *Optics Communications*, Vol. 246, 303, 2005.
5. Zhang, X. and X. Wang, *Optics & Laser Technology*, Vol. 37, 167, 2005.
6. Rostami, A. and M. S. Oskouei, *Optics communications*, Vol. 27, 4131, 2007.
7. Oskouei, M. S., S. Makouei, A. Rostami, and Z. D. K. Kanani, *Applied Optics*, Vol. 46, 6330, 2007.
8. H. Shahoei, H. Ghafoori-Fard, and A. Rostami, "A novel design methodology of multi-clad single mode optical fiber for broadband optical networks," *Progress In Electromagnetics Research*, PIER 80, 253–275, 2008.
9. Singh, S. P. and N. Singh, "Nonlinear effects in optical fibers: Origin, management and applications," *Progress In Electromagnetics Research*, PIER 73, 249–275, 2007.
10. Rostami, A. and A. Andalib, "A principal investigation of the group velocity dispersion (GVD) profile for optimum dispersion compensation in optical fibers: A theoretical study," *Progress In Electromagnetics Research*, PIER 75, 209–224, 2007.
11. Andalib, A., A. Rostami, and N. Granpayeh, "Analytical investigation and evaluation of pulse broadening factor propagating through nonlinear optical fibers (traditional and optimum dispersion compensated fibers)," *Progress In Electromagnetics Research*, PIER 79, 119–136, 2008.
12. Tripathi, R., R. Gangwar, and N. Singh, "Reduction of crosstalk in wavelength division multiplexed fiber optic communication systems," *Progress In Electromagnetics Research*, PIER 77, 367–378, 2007.
13. Ghosh, G., *Applied Optics*, Vol. 23, 976, 1984.
14. Kato, T., M. Hirano, A. Tada, K. Fokuada, T. Fujii, T. Ooishi, Y. Yokoyama, M. Yoshida, and M. Onishi, *Optical Fiber Technology*, Vol. 8, 231, 2002.
15. Agrawal, G. P., *Fiber-Optic Communication Systems*, John Wiley & Sons, 2002.